Supplementary Information: Low-Frequency Electrochemical Pulsing to Manage Flooding and Salt Precipitation in Zero-Gap CO2-to-Ethylene Electrolyzers

Michell Marufu[1,4U], Maxwell Goldman[1,4U, *], R. Dominic Ross[1,4,U], JongMin Lee[2], Jack Davis[3], Michael Troska[3], Eric Krall[1], Auston Clemens[3,4], Aditya Prajapati[1,4], Andrew Wong[3,4], Pavel Trtik[2], Abel Chuang[5], Eric Duoss[3], Sarah Baker[1,4], Christopher Hahn[1,4*].

[1]Materials Science Division, Lawrence Livermore National Laboratory, 7000 East Avenue, Livermore, CA, 94550 USA

[2]PSI Center for Neutron and Muon Sciences, 5232 Villigen PSI, Switzerland

[3]Materials Engineering Division, Lawrence Livermore National Laboratory, 7000 East Avenue, Livermore, CA, 94550 USA

[4]Laboratory for Energy Applications for the Future (LEAF), Lawrence Livermore National Laboratory, Livermore, CA 94550, USA

[5]Department of Mechanical Engineering, University of California, Merced, Merced, CA 95343, USA

[U] First authors

* Corresponding authors

Supplementary Figures

Figure S1. Postmortem of cathode flow fields after CO_2RR test showing extensive precipitation after continuous operation at 200mA/cm^2.

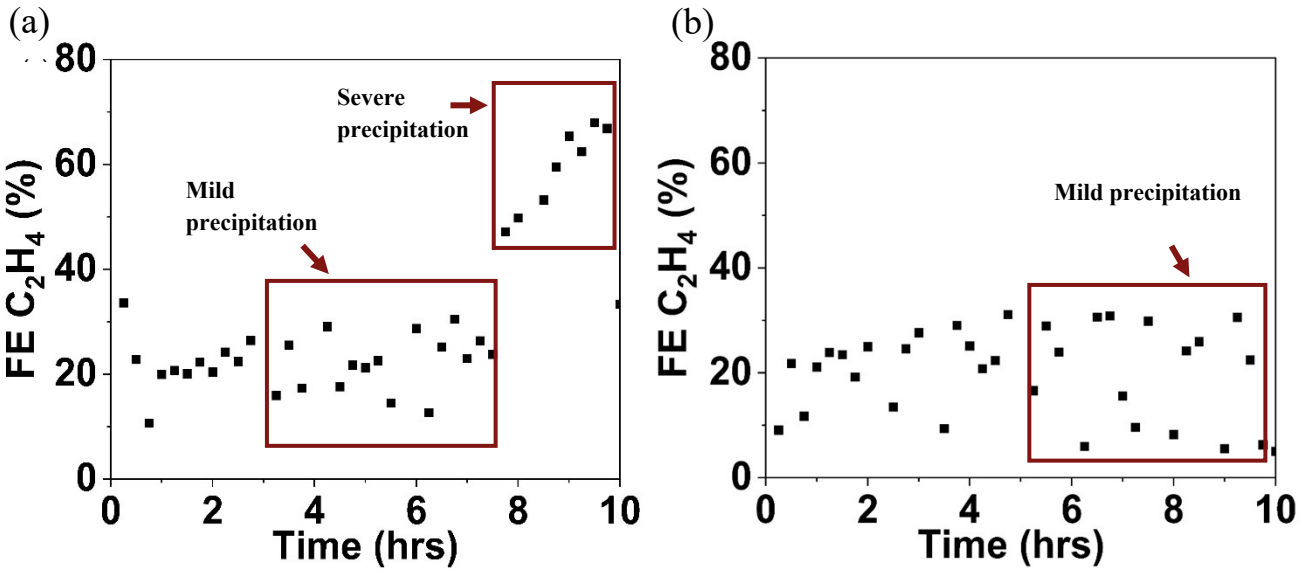

Figure S2: Ethylene Faradaic with modifications to t_R

(a) 45/5 -minute pulse. Steady operation is observed in the first three hours. Between the hours of 3 and 8, fluctuations in faradaic efficiency suggest the onset of mild precipitations. After 8 hours, severe precipitation is observed, with the dramatic increase in Faradaic efficiency resulting as an artifact of low gas flow rates caused by physical blockages in the gas diffusion layer and in the gas flow channels. (b) 45/10-minute pulse. Steady operation is observed for the first 4.5 hours, followed by precipitation.

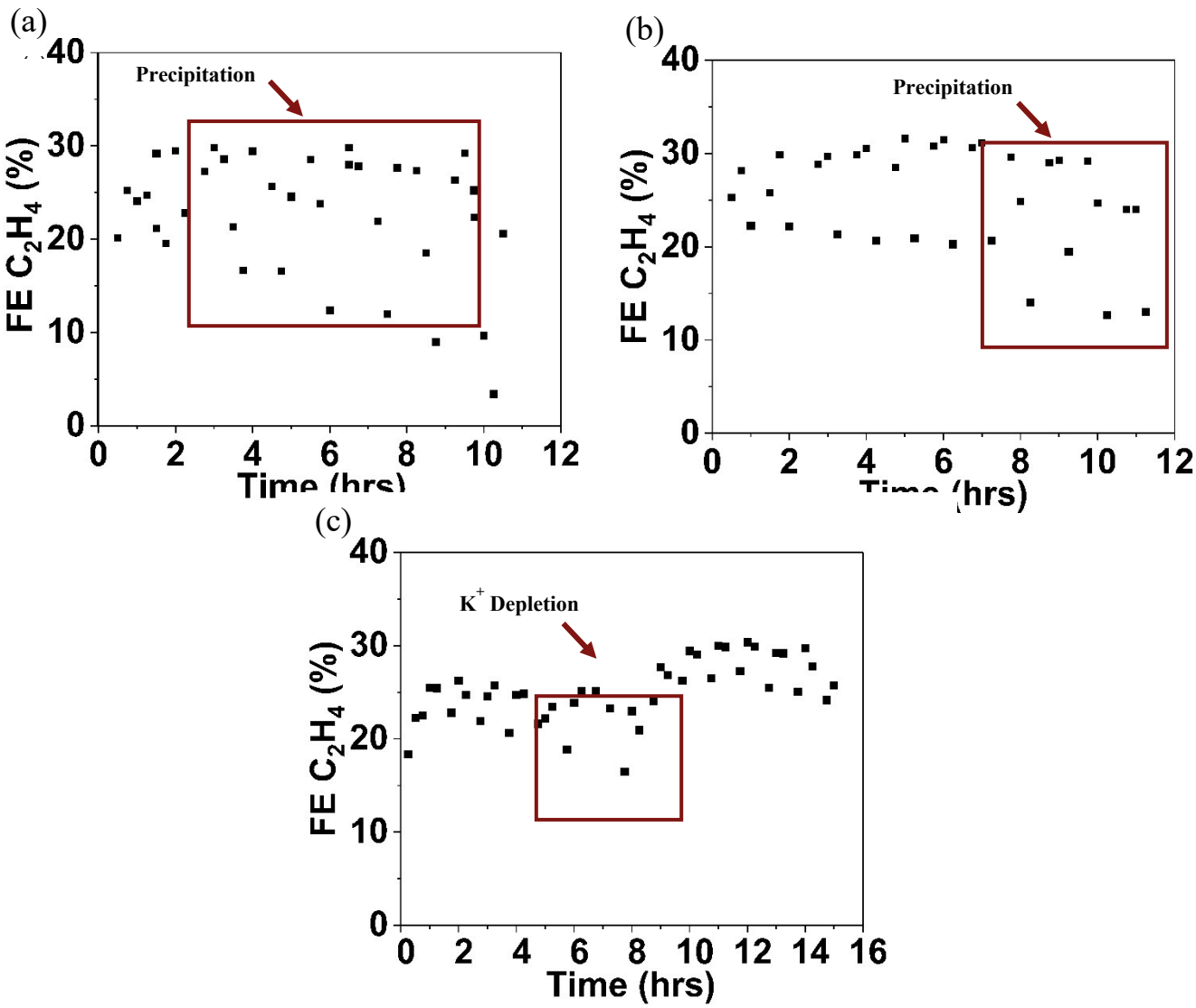

Figure S3: **Ethylene Faradaic Efficiency with J_P Modifications**

(a)Pulsing between 200 and 100 mA/cm² with a 45/15-minute cycle shows steady-state faradaic efficiency during the first 2 hours. After 2 hours, fluctuations become apparent, indicating the onset of precipitation, which increases in severity over time. (b) Pulsing between 200 and 50 mA/cm² with the same 45/15-minute timing maintains steady-state efficiency for a longer duration of 6.5 hours, after which precipitation begins to occur. (c) Pulsing between 200 and 20 mA/cm² with a 45/15-minute cycle shows in no observable precipitation. Instead, a gradual decline in overall faradaic efficiency is noted. An anolyte exchange at the 8-hour mark mitigates this decline, leading to a subsequent increase in efficiency.

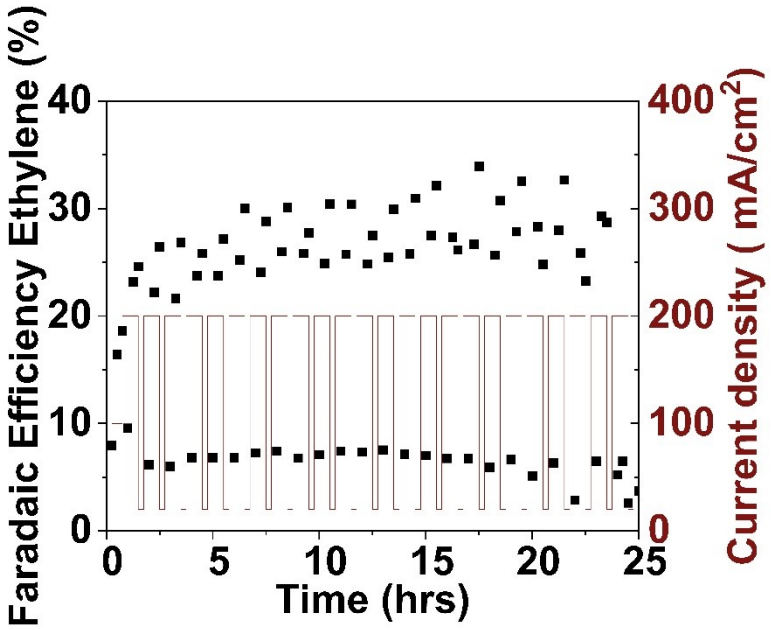

Figure S4: 25 hours test employing 200/20 mA/cm^2 pulsing sequence with 45/15-minute timing. Two anolyte swaps were carried out at 9 hours and at 23 hours. The 10-hour swap resulted in an uptick in $FE_{Ethylene}$ due to the reintroduction of K+ into the system. However, the anolyte swap at 23 hours resulted in precipitation due to membrane degradation resulting in higher levels of K^+ crossover necessitating an adjustment to either the pulsing sequence or the timing to better manage salt crossover.

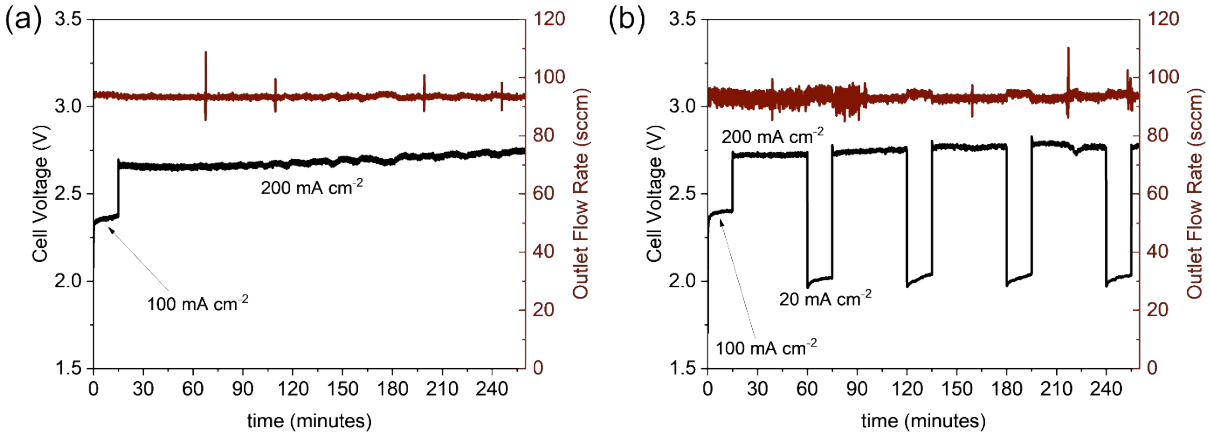

Figure S5. Full cell voltages and gas outlet flow rates of the electrolyzer during *operando* neutron radiography.

(a) After a 15-minute, 100 mA/cm^2 preconditioning current density, electrolyzer operated at 200 mA/cm^2 constant current. (b) after a 15-minute, 100 mA/cm^2 preconditioning current density, electrolyzer operated with a current pulse of 200/20 mA/cm^2 J_P/J_R, and 45/15-minute t_P/t_R.

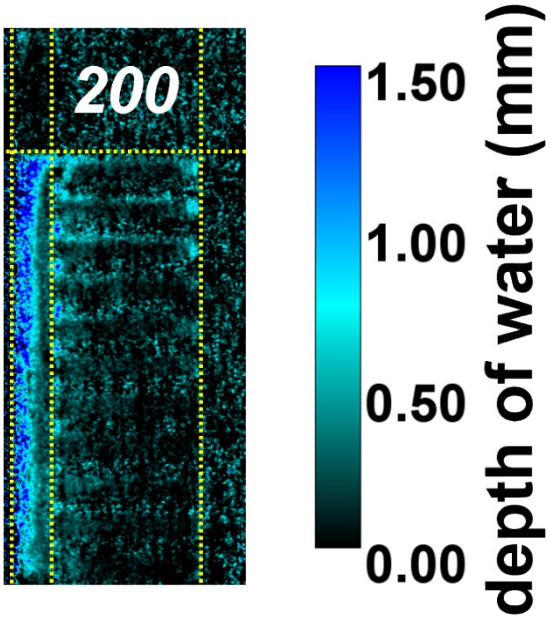

Figure S6. Additional J_R pulse after 255 minutes from the test shown in Figure S4.

Methods

Ionomer Synthesis

Chloromethylation of PPO, (CPPO): PPO (8.0 g, 66.6 mmol) was dissolved in 500 mL of $CHCl_3$ in a 1 L round bottom flask equipped with a stir bar. The reaction vessel was brought to 40 °C. 0.75 mL SnCl4 (1.69 g, 6.5 mmol) was added followed by dropwise addition of 40 mL TCMS (50.8 g, 339.8 mmol). Aliquots of the reaction solution were taken out at 3.2, 4.2, 6 and 7 hours. The polymer solutions were precipitated in 2x the amount in methanol and stirred for 30 minutes to ensure the absence of undesired side reactions that result in unwanted gelation, which can occur in PPO chloromethylation.[1] Precipitated CPPO was then filtered and washed 3 times with methanol. CPPO was dried in a vacuum oven at 50 °C for 24 h.

Quaternization of PPO: 2.0 g CPPO (30.0 mmol) was added to a 150 mL round bottom flask equipped with a stirring bar and dissolved in 65 mL NMP to yield a 3 wt% solution. The resulting mixture was heated at 40 °C, treated with 2.55 mL of 3.2 M TMA/MeOH

(8.15 mmol, 200% excess) and stirred for 42 h at 70 °C. Without further workup, the ionomer solution was casted into Teflon molds to achieve a solid ionomer. Ionomer solutions were then prepared by dissolving the ionomer in DMF, filtering through a 1 Um syringe filter, and diluting with IPA to achieve an 80:20 wt% of IPA to DMF at a concentration of 150mg/100mL of solution. [2]

Gas diffusion electrode fabrication

Gas diffusion electrodes were fabricated by spraying a sonicated mixture of copper nanoparticles (Sigma Aldrich, 25 nm, 2.5 mg/cm^2, weighed on a METTLER TOLEDO ME204E scale) and ionomer (IC ratio 0.3, powder weight) dissolved in an 8:2 IPA: DMF solvent onto a copper catalyst layer supported on Sigracet 39BB. The ink was sprayed onto the gas diffusion layer using a SONO-TEK Exacta-Coat system with an ultrasonic nozzle set 20 mm above the substrate, at 0.5 mL/min and 65 °C. During spraying, the sonic syringe prevented nanoparticle settling. Each sample was coated individually, with a purge step and a minimum 30-second dwell time before each spray. After coating, electrodes were dried overnight in the instrument prior to experimentation.

Materials

Gas diffusion electrodes were prepared using the methodology described above and cut into 5cm^2 geometric surface area. Carbon and titanium blocks printed each with a serpentine flow field (Fuel Cell Technologies Inc.) were utilized as the cathode and anode respectively. The flow field dimensions on each block were sized to the geometric surface area of the GDE. Each block also contained two pinholes to assist with alignment during assembly. Polytetrafluoroethylene (PTFE) gaskets (Grainger) were cut using a die press (Ace Steel Rule Dies) with holes sized to fit the area of the GDE. The gasket thicknesses utilized were 10/1000” thick. Anion exchange membranes (Sustianion, X37-50 Grade RT) were prepared, per manufacturer instructions, by cutting sheets sized to the anode and cathode blocks, soaking them in 1 M potassium hydroxide for at least 12 hours, with the solution replaced after 5 hours. When using PiperION® Anion Exchange Membrane (20 microns, Self-Supporting), the membrane was used as received from manufacturers and assembled dry.

Prior to assembly, alignment holes were cut into the membrane using a hole punch. Ni foam (MTI Corporation, 1.6mm thickness) was hot pressed to 10/1000” thick at 175 F, 20,000 psi for 5 minutes. Electrolyte was prepared using MilliQ water and potassium hydroxide (Sigma Aldrich, ACS Reagent, ≥85% pellets). Fuel Cell Technologies Inc, current collectors and electrolyzer housing were utilized. A torque wrench was used to tighten the screws (90 psi) to secure the assembly and adjust the assembly pressure. Carbon dioxide gas (Airgas, 99.999% purity) was used as received.

Electrolyzer Setup

MEAs were assembled by sequential layering of the electrode and membrane components, while the compression of the device was adjusted using a torque wrench. Electrolyte was then circulated through the anode side of the MEA by connecting the anode side flow field to an electrolyte reservoir, while the flow rate was controlled using a peristaltic pump (Cole Palmer). Carbon dioxide gas was input through the cathode compartment and output to a gas chromatograph (SRI Instruments) using a mass flow controller (MKS Instruments) to control the rate of gas delivery. The flow rate was monitored and controlled using a mass flow meter (Agilent and Omega).

Electrolysis

Electrolysis experiments were conducted in a two-electrode setup and controlled using a Biologic potentiostat (VSP-3e) configured with a booster (VMP 3B-20). All experiments were conducted with an initial break-in current of 100mA/cm^2 for 30-45 minutes. For the baseline experiments, this was followed by continuous operational current at 200mA/cm^2, and for the pulsed current experiments, the current was pulsed between a lower current, and the operational current density of 200mA/cm^2.

Gaseous products quantification

Gas chromatography (GC) was performed to detect CO_2RR products such as CO, CH_4, and C_2H_4 along with H_2 from the parasitic HER using an SRI GC 8610C MG#5 with a flame ionization detector (FID) and a thermal conductivity detector (TCD). A 3' MolSieve column was used to separate H_2 and CO from the gas mixture in tandem with 6' HaySep D column to separate the remaining gases- CO_2, CH_4, and C_2H_4. N_2 (research grade) was used as the carrier gas at 15 psi. H_2 (research grade) was set to 20 psi along with internal compressed air at 5 psi to ignite the flame for FID to detect hydrocarbons. A temperature profile was set for fast separation of the gaseous products starting with 50 C for 4.5 mins and then a temperature ramp to 200 C for 5.5 mins. A total runtime of 10 mins with 5 mins of cooldown time for GC was used for continuous measurements during the electrochemical experiments.

Neutron Radiography

Neutron radiography images were conducted at the Neutron Transmission Radiography (NEUTRA) beamline of the Swiss Spallation Neutron Source at the Paul Scherrer Institute.[3] Electrolysis was conducted with a similar setup to benchmarking, but to allow for transmission of neutrons through the cell, an all titanium electrolyzer (with a 3 cm^2 parallel flow field) was used. 10 mil thick PTFE gaskets were used on the anode and cathode side. To avoid K^+ depletion in the electrolyte over ~4-hour measurements, 500 mL of 0.5 M KOH was circulated through the anolyte chamber. Sustainion membranes

were stored in 0.5 M KOH until immediately before cell assembly, and the cell was assembled and transported to the beamline, with the anolyte circulation beginning within 15 minutes of the membrane being removed from the storage solution.

After mounting the cell at the beamline, the cell was heated to 40 °C. An initial "dry" image was taken of the cell while flowing 100 sccm of CO_2 without humidification. Afterwards, the humidification was turned on (also set to 40 °C at a bottle and 40 °C through a custom 10 foot heated line). Importantly, the humidification source was D_2O which provided more contrast for water crossing from the anolyte as opposed to condensed water from the humidified stream.

The imaging setup used a gadolinium oxysulfide (Gd_2O_2S) tilted scintillator coupled with an Andor Ikon-L charge-coupled-device (CCD) camera (Oxford Instruments) and Makro-Planar T* 2/100 lens (Zeiss).[4] The resulting effective spatial resolution was 20 μm in plane and 60 μm through plane using an exposure time of 30 s per image. Frames were averaged together over the entirety of each current step.

Operando images were processed using an in-house Python package that corrected for dark current, open beam, white spot filtering, beam current fluctuations, image registration, scattered background, referencing, and alignment.[5] Each image was normalized to the dry image. Absolute quantities of water (i.e. average path length of water that the beam passed through in the electrolyzer) was obtained by the following equation:

$$\text{image}_{\text{water}}\ (\text{mm}) = -\frac{1}{0.35} \bullet ln(image_{normalized}) = -\frac{1}{0.35} \bullet ln\left(\frac{image_{operando}}{image_{dry}}\right)$$

Where 0.35 represents a calibration constant for water previously obtained at NEUTRA. [6]

Determination of free K^+ with Potassium ion selective probe

K^+ concentration was determined by a Cole Parmer Double-Junction Potassium Ion-Selective Electrode (ISE) with a BNC connector (Item # UX-27502-39). This electrode operates by measuring a potential difference across a potassium selective membrane when immersed in a solution.[7] The measured potential is directly related to the activity of the potassium ions according to the Nernst equation. The potential (E) generated is proportional to the logarithm of the potassium ion activity. All measurements were taken at room temperature.

$$E = E_0 \frac{RT}{zF} \ln\ aK^+$$

Where:

- E Measured electrode potential (volts)
- E_0 Standard electrode potential (volts)
- R Universal gas constant (8.314 $J \cdot mol^{-1} \cdot K^{-1}$)
- T Temperature (Kelvin)
- z Charge of the ion (for K^+, z=1)
- F Faraday constant (96485 $C \cdot mol^{-1}$)
- aK^+ Activity of potassium ions in solution

Prior to analysis, the electrode was calibrated with standards of 1.95 ppm, 19.5 ppm and 195.5 ppm KOH solutions, generating a calibration curve. The first test pulsed between the primary current density (J_P) and reduced current densities (J_R) between 10-50mA/cm^2. The second test pulsed between the primary current density (J_P) and reduced current densities (J_R) between 50-90mA/cm^2. The test samples were diluted 1000-fold to ensure they fell within the ISE probe's operational pH range of 2-12. The measured potentials from the test samples were then compared to the calibration curve to determine their potassium concentrations before and after each test.

(a)

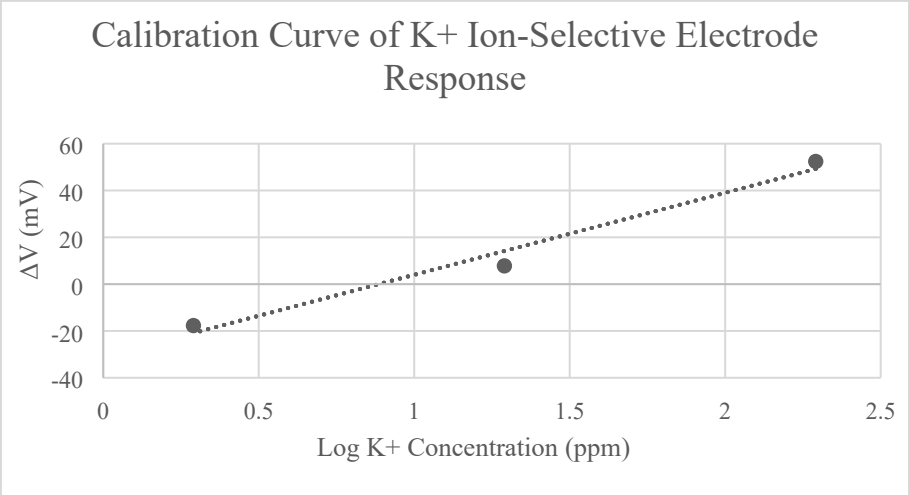

(b)

Solution	K^+ concentration in diluted sample	X1000 (Dilution compensation in ppm)	Difference in K^+ concentration
50-90mA/cm² Fresh Aliquot before test	10.61	10614.28	5727.13
50-90mA /cm² Aliquot after test	4.88	4887.15	
10-50mA/cm² Fresh Aliquot before test	5.15	5151.00	359.27
10-50mA/cm² Aliquot after test	4.79	4791.72	

Test pulsing sequence	Δ K^+ Concentration (ppm) before and after test
50-90mA /cm²	5727.13
10-50mA /cm2	359.27

Figure S7 (a) Calibration curve for potassium concentration determination using KOH solutions of known ppm concentrations (b) Determination of K+ concentration (ppm) in samples from 10-50mA/cm² pulsing sequence and 50-90mA/cm² sequence.

$y = 35.032x - 31.039$

log conc = (potential + 31.039)/35.032

Author Contributions

M.M and M.G. conceptualized the project and designed the methodology. M.M, M.G., and D.R. wrote the original draft M.M., M.G. D.R., and J.L. carried out all experiments, M.M., M.G, D.R. and A.W. analyzed data, contributed to the discussion, and prepared the manuscript. C.H., S.B., and E.D. edited the manuscript. E.K. and A.C. prepared the Gas Diffusion Electrodes. M.G, E.D, S.B, C.H supervised the project.

Acknowledgements

This material is based upon work supported by the U.S. Department of Energy's Office of Energy Efficiency and Renewable Energy (EERE) under the Advanced Manufacturing Office (AMO) funding opportunity announcement DE-FOA-0002252. This work is based on experiments (beamtime proposal No. 20240011) performed at the Swiss spallation neutron source SINQ, Paul Scherrer Institute, Villigen, Switzerland. M.M., M.G., D.R., J.D., M.T., E.K., A.W., E.D., S.B., C.H. contributed under the auspices of the US Department of Energy by Lawrence Livermore National Laboratory under contract DE-AC52-07NA27344 and was supported by CRADA TC02449 and Laboratory Directed Research and Development (LDRD) under project 22-SI-006 Funding was also provided by U.S. Department of Energy Office of Energy Efficiency and Renewable Energy Bioenergy Technologies Office . The U.S. Government retains, and the publisher, by accepting the article for publication, acknowledges that the U.S. Government retains a nonexclusive, paid-up, irrevocable, worldwide license to publish or reproduce the published form of this work, or allow others to do so, for U.S. Government purposes.

(1) Feng, Z.; Esteban, P. O.; Gupta, G.; Fulton, D. A.; Mamlouk, M. Highly Conductive Partially Cross-Linked Poly(2,6-Dimethyl-1,4-Phenylene Oxide) as Anion Exchange Membrane and Ionomer for Water Electrolysis. *International Journal of Hydrogen Energy* **2021**, *46* (75), 37137–37151. https://doi.org/10.1016/j.ijhydene.2021.09.014.
(2) Goldman, M.; Prajapati, A.; Cross, N. R.; Clemens, A.; Chu, A. T.; Gutierrez, L.; Marufu, M.; Krall, E.; Ehlinger, V.; Moore, T.; Duoss, E. B.; Baker, S. E.; Hahn, C. Designing Ionomers to Control Water Content for Low-Voltage Ethylene Production from CO2 Electrolysis. *Chem Catalysis* **2025**, *0* (0). https://doi.org/10.1016/j.checat.2025.101497.
(3) LEHMANN, E. H.; VONTOBEL, P.; WIEZEL, L. Properties of the Radiography Facility Neutra at Sinq and Its Potential for Use as European Reference Facility. *Nondestructive Testing and Evaluation* **2001**, *16* (2–6), 191–202. https://doi.org/10.1080/10589750108953075.

(4) Boillat, P.; Frei, G.; Lehmann, E. H.; Scherer, G. G.; Wokaun, A. Neutron Imaging Resolution Improvements Optimized for Fuel Cell Applications. *Electrochem. Solid-State Lett.* **2010**, *13* (3), B25. https://doi.org/10.1149/1.3279636.
(5) Boillat, P.; Carminati, C.; Schmid, F.; Grünzweig, C.; Hovind, J.; Kaestner, A.; Mannes, D.; Morgano, M.; Siegwart, M.; Trtik, P.; Vontobel, P.; Lehmann, E. H. Chasing Quantitative Biases in Neutron Imaging with Scintillator-Camera Detectors: A Practical Method with Black Body Grids. *Opt. Express, OE* **2018**, *26* (12), 15769–15784. https://doi.org/10.1364/OE.26.015769.
(6) Iranzo, A.; Boillat, P.; Rosa, F. Validation of a Three Dimensional PEM Fuel Cell CFD Model Using Local Liquid Water Distributions Measured with Neutron Imaging. *International Journal of Hydrogen Energy* **2014**, *39* (13), 7089–7099. https://doi.org/10.1016/j.ijhydene.2014.02.115.
(7) Vidal-Iglesias, F. J.; Solla-Gullón, J.; Rodes, A.; Herrero, E.; Aldaz, A. Understanding the Nernst Equation and Other Electrochemical Concepts: An Easy Experimental Approach for Students. *J. Chem. Educ.* **2012**, *89* (7), 936–939. https://doi.org/10.1021/ed2007179.